

## RE-CIRCULATING LINAC VACUUM SYSTEM\*

R.P. Wells, J. N. Corlett, A.A. Zholents, LBNL, Berkeley, California 94720, USA

### Abstract

The vacuum system for a proposed 2.5 GeV, 10 $\mu$ A re-circulating linac synchrotron light source [1] is readily achievable with conventional vacuum hardware and established fabrication processes. Some of the difficult technical challenges associated with synchrotron light source storage rings are sidestepped by the relatively low beam current and short beam lifetime requirements of a re-circulating linac. This minimal lifetime requirement leads directly to relatively high limits on the background gas pressure through much of the facility. The 10 $\mu$ A average beam current produces very little synchrotron radiation induced gas desorption and thus the need for an “ante-chamber” in the vacuum chamber is eliminated. In the arc bend magnets, and the insertion devices, the vacuum chamber dimensions can be selected to balance the coherent synchrotron radiation and resistive wall wakefield effects, while maintaining the modest limits on the gas pressure and minimal outgassing.

### INTRODUCTION

The baseline electron beam current is 10  $\mu$ A (1nC/bunch at 10kHz) at an energy of 2.5GeV. However, to allow for potential upgrades to the design, the vacuum system is designed for 30  $\mu$ A at 3.1 GeV. The bunch length is compressed from 20 ps at the cathode to 2 ps at the exit of the arc connecting the pre-accelerator to the re-circulating linac (Arc 0). The 2 ps bunch length is then held constant throughout the re-circulating sections. Note “Arc” as used throughout this section refers to entire circulation path at a given energy, straight sections as well as arcs at the ends of the straight sections. This present study considers the vacuum issues associated primarily with the bend sections of the lattice. The vacuum requirements of the electron gun, linac, undulators and beamlines will be addressed in future studies.

The design of vacuum systems for synchrotron radiation sources must consider several possible physical processes to establish the allowable background gas partial pressures and chamber dimensions including;

- Beam loss due to interaction with background gas by
  - inelastic scattering of the beam by gas nuclei and
  - large angle elastic scattering by gas nuclei.
- Energy loss, resulting in longitudinal emittance growth due to coherent synchrotron radiation (CSR)
- Transverse emittance growth due to resistive wall wakefields

To reduce the effects of CSR, the vacuum chamber aperture is reduced to shield against emission of longer

wavelength radiation [2,3]. This has the effect of producing a higher cut-off frequency for the radiation propagating within the vacuum chamber and may be selected to narrow the frequency spectrum of coherent emission from a bunch. The coherent radiation emission process is then effectively suppressed. The CSR effect is present only in the bend magnets, and a larger aperture may be employed elsewhere.

The resistive wall wakefield generated by the electron beam traveling in a vacuum chamber of finite conductivity, is proportional to the chamber length and inversely proportional to both the square root of the chamber’s electrical conductivity and the cube of the chamber’s half-height. The resistive wall effect therefore has implications on the choice of vacuum chamber material, the minimum chamber height and the location tolerance of the chamber with respect to the beam axis.

The final chamber geometry, and most importantly the chamber inner height, will be determined by selecting an appropriate compromise between reducing CSR effects, resistive wall effects, and beam loss due to collisional scattering with background gas. An example of this compromise is the plot of the CSR energy loss and transverse resistive wall distortion as a function of chamber height shown in Figure 1. These affects are different for each beam pass due to the different beam energy and magnet bend radii, the optimal chamber height is therefore different for each arc. From an analysis of collective effects [2,3] a minimum vacuum chamber height of between 7 and 9 mm is indicated.

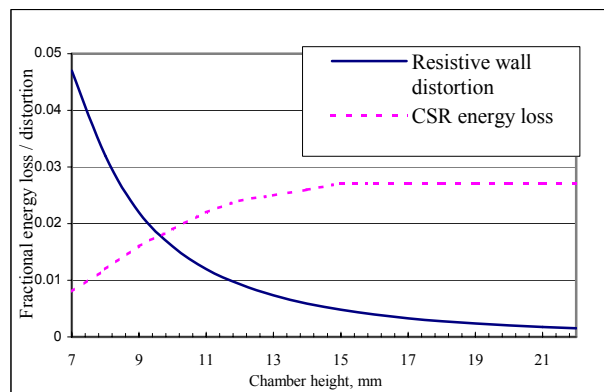


Figure 1. Comparison of energy loss due to CSR and beam distortion from resistive wall effects.

Since the actual combined collective effects is still under study, the selected beam chamber heights are preliminary estimates only.

\* This work supported by the U.S. Department of Energy under Contract No. DE-AC03-76SF00098

## BEAM LOSS

In storage ring type synchrotron light sources, beam-gas scattering may be one of the prime limitations on beam lifetime and hence allowable background gas pressures. The beam lifetime requirement for the re-circulating linac configuration is extremely modest due to the relatively small, 900 meter, total path length (or equivalently,  $\sim 3\mu\text{s}$  time of flight).

Charged particles passing through matter become deflected by the strong electric fields of the nucleus. This deflection constitutes a transverse acceleration of the particle and results in a loss of energy through Bremsstrahlung radiation. If the energy loss exceeds the energy acceptance of the accelerator,  $\delta_{\text{acc}}$ , the particle is lost. Following the methodology of Wiedemann [4] and assuming a conservative energy acceptance fraction of  $\delta_{\text{acc}} = 0.001$ , the Bremsstrahlung lifetime for residual gas pressures from  $10^{-4}$  to  $10^{-8}$  Torr is 0.8 – 8,000 seconds. While admittedly short by storage ring standards, this is well in excess of re-circulating linac requirements

An electron passing through background gas may also experience an elastic collision (Coulomb scattering) that causes an angular deflection large enough to give the particle a betatron oscillation amplitude larger than the limiting physical or dynamic aperture of the accelerator. For planning purposes, and to be consistent with the collective beam effects discussed above, a limiting physical rectangular aperture of 9mm high by 40mm wide was assumed. In accordance with good practice, we assume that the dynamic aperture will exceed the physical aperture throughout the accelerator.

For the present study, an average betatron function in the bend sections of 30 m was selected based on 150% of the MAD output for the lattice. A “worst-case” local betatron function of 90 m was selected based on the highest value found anywhere in the lattice. The beam lifetime and consequently the beam loss was calculated using the equation for a rectangular aperture from Turner [5]. Beam losses of less than 0.1% are expected at average pressures up to  $2 \times 10^{-6}$  Torr. Commensurate with the modest beam losses, the power deposition on the vacuum chamber due to scattering is relatively insignificant for residual gas pressures as high as  $10^{-5}$  Torr.

## VACUUM SYSTEM LAYOUT

The vacuum system must accommodate the magnet lattice as well as the various collective beam effects. With the exception of the first arc and the spreader regions, the lattice consists primarily of identical dipole, quadrupole and sextupole magnets. Pole gaps in the dipoles are 30 mm (full height) while the diametric clearance of the quadrupoles and sextupoles is greater than 60 mm. These magnets set the maximum external dimensions of the beam tube throughout the accelerator. Collective beam effects dictate the inner height of the vacuum chamber within bend magnets.

As with any vacuum system, the pressure is determined by the amount of gas introduced, the

conductance of the gas to the pumps and the pump speed. The gas load is a product of thermal outgassing and photon induced desorption.

The amount and mixture of gas liberated from the vacuum wall is a function of the material selected and its preparation. For the purposes of this study, a vacuum baked ( $150^\circ\text{C}$ –24 hrs.) aluminum beam tube and “conflat” type metal sealed fittings are assumed.

The proposed vacuum system consists of an extruded rectangular beam tube in the bend magnet locations transitioning to a circular tube in the straight sections. The internal height of the rectangular tube may vary with each arc as determined by collective effects described previously. The beam tube is connected periodically to a large diameter aluminum pipe that serves as a pumping manifold. A series of modular cryosorption pumps are distributed along the manifold to provide the primary pumping. A small number of turbomolecular pumps backed by oil-free roughing pumps will provide the initial system vacuum and cryopump regeneration.

The proposed system contains several variables that can be optimized based on the conditions within a given region of the accelerator. These variables include the width of the beam tube, spacing between manifold-beam tube connections, manifold diameter and cryopump spacing. While each portion of the accelerator section will behave differently, of primary concern are the bend magnets where gas production is the greatest and gas conductance is the least.

## OUTGASSING

The equations derived by Mathewson, et.al. [6] were used to calculate outgassing rates due to synchrotron radiation. Gas is desorbed from the beam tube surface by thermal processes and by synchrotron radiation induced photoelectrons. The number of photoelectrons produced per meter of vacuum chamber range from zero in the injection arc to  $6 \times 10^{14}$  in the final arc. Calculated gas desorption rates, using species specific desorption efficiencies [7],  $\eta$ , are shown in Table 1.

Table 1. Desorption rates per meter of beam tube.

| Gas             | $\eta$ | $Q_{\text{pe}}$ (Torr-liter/sec-m) |                      |                      |                      |                      |
|-----------------|--------|------------------------------------|----------------------|----------------------|----------------------|----------------------|
|                 |        | Arc 0                              | Arc 1                | Arc 2                | Arc 3                | Arc 4                |
| H <sub>2</sub>  | 0.1    | -                                  | $1.9 \times 10^{-6}$ | $2.3 \times 10^{-6}$ | $3.1 \times 10^{-6}$ | $3.3 \times 10^{-6}$ |
| CO              | 0.03   | -                                  | $5.8 \times 10^{-7}$ | $6.8 \times 10^{-7}$ | $9.2 \times 10^{-7}$ | $1.0 \times 10^{-6}$ |
| CO <sub>2</sub> | 0.025  | -                                  | $4.8 \times 10^{-7}$ | $5.7 \times 10^{-7}$ | $7.6 \times 10^{-7}$ | $8.3 \times 10^{-7}$ |
| CH <sub>4</sub> | 0.008  | -                                  | $1.5 \times 10^{-7}$ | $1.8 \times 10^{-7}$ | $2.4 \times 10^{-7}$ | $2.7 \times 10^{-7}$ |
| Total           |        |                                    | $3.1 \times 10^{-6}$ | $3.7 \times 10^{-6}$ | $5.0 \times 10^{-6}$ | $5.4 \times 10^{-6}$ |

The power deposition on the vacuum tube wall from synchrotron radiation, estimated from emission of an electron beam in uniform circular motion [8], is  $5.4 \times 10^{-3}$  W/cm with a negligible peak flux is of  $0.5 \text{ W/cm}^2$ .

The quantity and composition of thermally desorbed gas is substantially altered by a moderate vacuum bake-out in aluminum systems. After baking the amount of

thermal outgassing is more than 6,000 times smaller than synchrotron radiation induced desorption.

### GAS PRESSURE PROFILE

The most difficult pumping conditions are present in the arc sections due to the limited gas conductance and the synchrotron radiation induced gas load. The pumping of the straight sections is relatively straightforward in comparison and is not considered in this study. Given the assumption of a discretely pumped system, a rational configuration would include widely spaced pumps, a manifold sized to be consistent with the pump size and a limited number of beam tube penetrations. A system that meets the criteria consists of CTI-8 cryopumps centrally located on a 10 m span of 20 cm diameter manifold. Short, 30 cm long by 5 cm diameter tube and bellows assemblies connect the manifold to the beam tube. A representative section of the system is illustrated in Figure 2 and shown schematically in Figure 3.

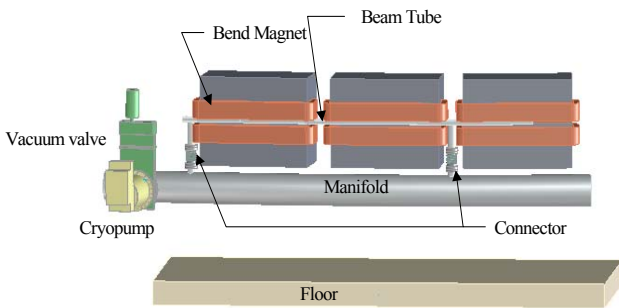


Figure 2. Section of Arc 4 vacuum system.

In addition to the outgassing rate, the pressure in the beam tube is a function of the gas conductance and pump speed. For ease of computation, gas evolved from the beam tube, connector tubing and manifold is treated as a single continuous distributed source along the length of the manifold. The conductance of the cylindrical tubing was calculated using Santeler's [9] correction to the common formula for a circular tube in molecular flow.

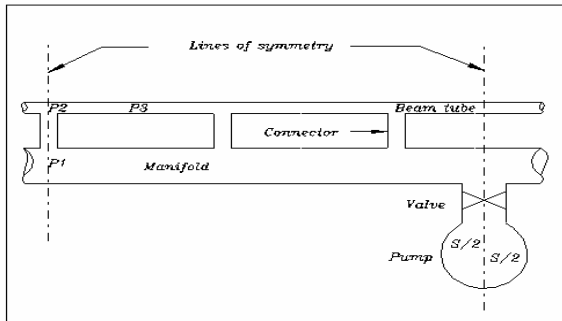


Figure 3. Schematic of a typical vacuum system section.

The pressure at the connecting tube entrance, P2, is determined by adding the pressure differential from gas flow through the connecting tube to the maximum pressure in the manifold, P1. The peak pressure in the

beam tube, P3, is found by adding the maximum pressure increase along the beam tube, between connectors, to the pressure at the connector entrance, P2. The conductance of the beam tube is calculated using the equation from Roth [10] for a long rectangular tube of uniform cross section.

The plot shown in Figure 4 is an approximate pressure profile of the Arc 4 beam tube derived by applying the methodology used to find pressures P1-P3 to the other analogous positions along the beam tube and then applying a parabolic profile between them. By inspection, the average pressure along the path of the beam is  $3 \times 10^{-7}$  Torr. This residual gas pressure compares favorably with the pressure of  $\sim 10^{-6}$  Torr required to limit beam losses from scattering to 0.1%.

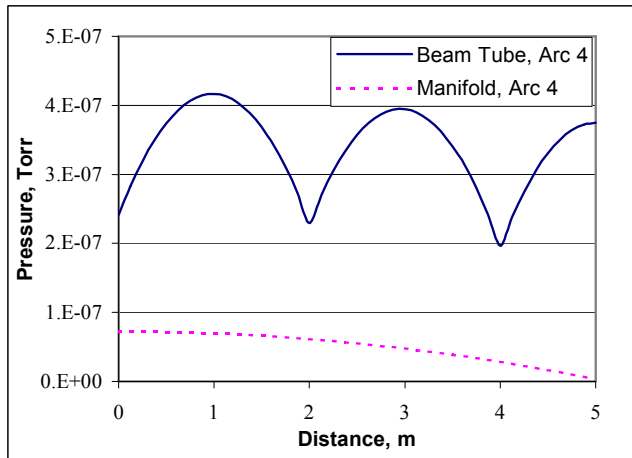


Figure 5. Pressure profile along a representative portion of the Arc 4 beam tube.

### REFERENCES

- [1] J.N. Corlett et al "A Recirculating Linac-Based Facility for Ultrafast X-ray Science", this conference
- [2] S. De Santis et al "Collective effects analysis for the Berkeley femtosource", this conference
- [3] A. Zholents et al, "Longitudinal phase-space control in the Berkeley Femtosecond X-ray light source", this conference.
- [4] H. Wiedemann, Particle Accelerator Physics I, pp.378-380
- [5] W.C. Turner, "Notes for a Course on Accelerator Vacuum Physics", CBP Tech. Note 188, June 11, 1999.
- [6] A.G. Mathewson, G.H. Horikoshi, and H. Mizuno, "Some Notes on the Photoelectron Induced Gas Desorption Problems in the Photon Factor and Tristan", National Lab for High Energy Physics Report, Japan.
- [7] M. Achard, "Electron and Ion Induced Gas Desorption from Stainless Steel, OFHC Copper, Titanium and Pure Aluminum", CERN-ISR-VA/76-34
- [8] PEP-II Conceptual Design Report, June 1993, p305.
- [9] D.J. Santeler, "New Concepts in Molecular Gas Flow", J.Vac. Sci. Tech. A, Vol.4, No.3, May/June 1986
- [10] Roth, Vacuum Technology 2<sup>nd</sup> Ed., North-Holland, 1982 pp.84-87.